1521-009X/45/5/576–580$25.00
DRUG METABOLISM AND DISPOSITION

https://doi.org/10.1124/dmd.116.074575
Drug Metab Dispos 45:576–580, May 2017

Novel Method to Predict In Vivo Liver-to-Plasma K_{puu} for OATP Substrates Using Suspension Hepatocytes

Keith Riccardi, Jian Lin, Zhenhong Li, Mark Niosi, Sangwoo Ryu, Wenyi Hua, Karen Atkinson, Rachel E. Kosa, John Litchfield, and Li Di

Pharmacokinetics, Dynamics and Metabolism, Pfizer Inc., Groton, Connecticut (K.R., Ji.L., M.N., S.R., W.H., K.A., R.E.K., L.D.); Cambridge, Massachusetts (Z.L., Jo.L.)

Received December 8, 2016; accepted March 1, 2017

ABSTRACT

The ability to predict human liver-to-plasma unbound partition coefficient (K_{puu}) is of great importance to estimate unbound liver concentration, develop PK/PD relationships, predict efficacy and toxicity in the liver, and model the drug-drug interaction potential for drugs that are asymmetrically distributed into the liver. A novel in vitro method has been developed to predict in vivo K_{puu} with good accuracy using cryopreserved suspension hepatocytes in InVitroGRO HI media with 4% BSA. Validation was performed using six OATP substrates with rat in vivo K_{puu} data from i.v. infusion studies where a steady state was achieved. Good in vitro-in vivo correlation (IVIVE) was observed as the in vitro K_{puu} values were mostly within 2-fold of in vivo K_{puu}. Good K_{puu} IVIVE in human was also observed with in vivo K_{puu} data of dehydropravastatin from positron emission tomography and in vivo K_{puu} data from PK/PD modeling for pravastatin and rosuvastatin. Under the specific K_{puu} assay conditions, the drug-metabolizing enzymes and influx/efflux transporters appear to function at physiologic levels. No scaling factors are necessary to predict in vivo K_{puu} from in vitro data. The novel in vitro K_{puu} method provides a useful tool in drug discovery to project in vivo K_{puu}.

Introduction

Liver is an important organ for many disease targets, such as dyslipidemia, diabetes, obesity, and nonalcoholic steatohepatitis. It is critical to understand the unbound drug concentration in the liver, because it impacts pharmacological activity, metabolic and biliary clearance, and DDI (Smith et al., 2010). For compounds that are not actively transported and are not influenced by membrane potential or pH gradient (Scott et al., 2016), the unbound drug concentration in the liver will be the same as that in the plasma. In this case, the unbound partition coefficient (K_{puu}) between liver and plasma is close to 1. When compounds are uptake transporter substrates (e.g., OATPs), K_{puu} values can be greater than 1 due to active influx. K_{puu} represents the distribution of unbound drugs between liver and plasma in vivo or between hepatocytes and media in vitro when multiple processes, including metabolism, uptake, efflux, and passive diffusion, have achieved a steady state. K_{puu} can be described using the extended clearance equation incorporating the multiple mechanisms (Shitara et al., 2006; Watanabe et al., 2010; Yabe et al., 2011). It is important to be able to estimate in vivo K_{puu}, since it is the link between unbound plasma concentration and unbound liver concentration. Because it is challenging to measure the unbound liver concentration directly in higher species (e.g., nonhuman primate) and humans, the ability to predict K_{puu} will enable direct estimation of unbound liver concentrations from unbound plasma concentrations.

Currently, several in vitro methods (Riccardi et al., 2016) are available to estimate K_{puu}, including the binding method (Mateus et al., 2013), the kinetic method (Yabe et al., 2011), and the temperature method (Shitara et al., 2013). However, validation of these methods with in vivo exposure/pharmacology or in vitro activity data are fairly limited (Shitara et al., 2013; Riccardi et al., 2016). IVIVE for K_{puu} using hepatocyte systems for OATP substrates has not been established. Several studies have shown internalization or downregulation of transporters in the hepatocyte systems (Roelofsen et al., 1995; Bow et al., 2008; Kimoto et al., 2012; Kunze et al., 2014; Morse et al., 2015; Vildhede et al., 2015), although others have shown no significant difference in transporter abundance between hepatocytes and liver tissues (Prasad et al., 2014; Badee et al., 2015). It is uncertain whether a direct translation is possible without scaling factors from in vitro hepatocytes to in vivo K_{puu}. In this study, we explored the IVIVE of K_{puu} using cryopreserved suspension rat and human hepatocytes for OATP substrates. The ability to predict in vivo liver-to-plasma K_{puu} from in vitro systems will provide a useful tool in drug discovery to predict unbound liver concentration as well as clearance and dose, to design drugs for liver targeting, to develop pharmacokinetic (PK)/pharmacodynamics (PD) relationships for disease targets residing in the liver, and model DDI due to inhibition/induction of liver enzymes when transporters are involved in the distribution processes.

Materials and Methods

Materials. Test compounds were obtained from obtained from Sigma-Aldrich (St. Louis, MO) or Pfizer (Groton, CT). PF-04991532 (Compound 19 in the reference) (Pfefferkorn et al., 2012) and PF-05187965 (Compound 7 in the

https://doi.org/10.1124/dmd.116.074575.
This article has supplemental material available at dmd.aspetjournals.org.

ABBREVIATIONS: BSA, bovine serum albumin; CI, confidence interval; DDI, drug-drug interaction; DHP, dehydropravastatin; DMSO, dimethylsulfoxide; f_u, fraction unbound; $f_{u,cell}$, fraction unbound of cells; $f_{u,liver}$, fraction unbound of liver; $f_{u,media}$, fraction unbound of media; $f_{u,p}$, fraction unbound of plasma; IS, internal standard; IVIVE, In vitro-in vivo extrapolation/correlation; K_p, partition coefficient; $K_{puu,}$, unbound partition coefficient; LC-MS/MS, liquid chromatography-tandem mass spectrometry; MVA, mevalonic acid; OATP, organic anion-transporting polypeptide; PBS, phosphate-buffered saline; PD, pharmacodynamics; PET, positron emission tomography; PK, pharmacokinetics; RT, room temperature.

reference) (Stevens et al., 2013) were synthesized according to the methods reported in the referenced publications. Rat plasma (from 14 males and 14 females, pooled) and human plasma (from 6 males, pooled), cryopreserved human hepatocytes (Lot DCM, custom-pooled of both male and female, 10 donors), and Wistar-Han rat hepatocytes (Lot VSU, 35 male pooled donors) were purchased from BioreclamationIVT, LLC (Hicksville, NY). Human liver (1 male donor) was from Analytical Biologic Services Inc. (Wilmington, DE). Wistar-Han rat liver (four male donors) was obtained internally at Pfizer Global Research and Development (Groton, CT). Williams' Medium E (catalog #C1984, custom formula number 91-5233EC; ThermoFisher Scientific, Waltham, MA) contained 26 mM sodium bicarbonate and 50 mM HEPES, InVitroGRO HI media, and M-PER buffer were purchased from ThermoFisher Scientific. BSA (free of fatty acid; catalog #A4612) and other reagents were from Sigma-Aldrich unless specified. The equilibrium dialysis device (96-well format) and cellulose membranes (molecular weight cutoff, 12,000–14,000) were obtained from HTDialysis, LLC (Gales Ferry, CT). Breathe Easy sealing membranes were obtained from Sigma-Aldrich.

Determination of Fraction Unbound. In preparation of in vitro fraction unbound (f_u) measurement, rat and human liver tissues were homogenized in PBS (1:5 tissue: PBS dilution) at RT with an Omni TH tissue homogenizer (Omni International, Kennesaw, GA). A probe (7 × 110 mm) was used for 30-second pulses at high speed. InVitroGRO HI media containing 4% BSA and plasma were used directly without any dilution for binding determination. Before an experiment, the dialysis membranes were soaked in water for 15 minutes, 30% ethanol/water for 15 minutes, and PBS for 15 minutes or overnight. The dialysis device was put together following the instructions from the manufacturer (http://www.htdialysis.com). Compound stock solutions were prepared at 200 μM in dimethylsulfoxide (DMSO), added to matrices (1:100 dilution), and mixed well with a multichannel pipettor (Eppendorf; VWR, Radnor, PA). The final test compound concentration for equilibrium dialysis was 2 μM with 1% DMSO. An aliquot (150 μL) of matrix (plasma, liver homogenate, or assay media) containing 2 μM test compound was added to the donor side of the membrane, and PBS (150 μL) was added to the receiver side of the membrane. The dialysis device was sealed with Breathe-Easy Membranes (Sigma-Aldrich). Quadruplicates were used for each compound in binding experiments. The dialysis device was incubated in a humidified incubator (75% relative humidity, 5% CO_2/95% air) at 37°C for 6 hours at 200 rpm with an orbital shaker (VWR). Alternative binding methods (before saturation or dilution) were also used for highly bound compounds to ensure that equilibrium had been achieved (Riccardi et al., 2015). After the incubation was completed, matrix samples (15 μL) from the donor wells were added to 45 μL of PBS in a 96-well plate. Dialyzed PBS (45 μL) from the receiver wells was added to the blank matrix (15 μL). Matrix material (15 μL) containing 2 μM compound from both before and after incubation was taken and added to 45 μL PBS in a 96-well plate. They were used to assess the recovery and stability of the samples. Cold acetonitrile (200 μL) containing internal standard (IS; a cocktail of 5 ng/ml terfenadine and 0.5 ng/ml tolbutamide) was added to all the samples for protein precipitation. The samples were vortexed for 3 minutes (VWR) and centrifuged at 3000 rpm for 5 minutes (Allegra 6R; Beckman Coulter, Fullerton, CA) at RT. The supernatant was transferred, dried down, reconstituted with solvents, and analyzed by LC-MS/MS. Sertraline was used on every incubation plate for quality control. Calculation of f_u has been discussed previously (Riccardi et al., 2015, 2016).

In Vitro K_{puu} Measurement. The cryopreserved hepatocytes were thawed and resuspended in William's Medium E. The number of cells and viability were determined using the Trypan Blue exclusion method. Cell suspensions were centrifuged (Allegra 6R; Beckman Coulter) at 50*g* at RT for 3 minutes. Media were removed and cells were resuspended in InVitroGRO HI media supplemented with 4% BSA. Test compounds (1 mM) were prepared in DMSO, and 1 μl was added to the suspended hepatocytes at 0.5 million cells/ml in 1 ml. The final compound concentration is 1 μM with 0.1% DMSO. Two to four replicates were used for each compound. The suspension was incubated at 37°C in a humidified incubator (75% relative humidity, 5% CO_2/95% air) with for 4 hours to ensure that the steady state was reached. At the end of the incubation, the cell suspension was centrifuged for 3 minutes at 500 rpm and supernatant was sampled to determine the medium concentration. The remaining medium was removed from the hepatocytes. The cells were washed with cold PBS three times (1 ml each time) and lysed with 75 μl M-PER buffer. The solution of the lysed cells was sampled for analysis. Cold acetonitrile with IS was added to both the supernatant and the cell-lysed solutions and mixed. The solution was centrifuged at 3000 rpm for 5 minutes at RT, and the supernatants were transferred for LC-MS/MS analysis using standard curves from both media and cells. Calculation of in vitro K_{puu} has been discussed previously (Riccardi et al., 2016). Here, $f_{u,cell}$ is replaced with $f_{u,liver}$ since the two values are quite comparable, as liver comprised of 80% hepatocytes by volume (Bayliss and Skett, 1996).

In Vivo Rat Liver-to-Plasma K_{puu} Determination. The i.v. infusion experiments in rats were conducted at BioDuro (Shanghai, People's Republic of China). Wistar-Han rats (male, $n = 3$, fed) were infused i.v. through a jugular vein cannula at a rate of 4–9 μl/min with test compounds using a programmable pump (Harvard 2000; Harvard Apparatus, Holliston, MA). The doses were selected based on the i.v. bolus data and the detection limit. Infusion time was determined using a duration greater than five times the terminal half-life that was predetermined from i.v. bolus data. Under this condition, K_{puu} should be close to steady state, because a greater than 97% steady state is achieved at five times the half-life (Ito, 2011; Hedaya, 2012). Dose and formulation of the compounds are summarized in Table 1. At the end of infusion, blood samples were obtained from the carotid artery catheter, and livers were also collected. Liver samples were rinsed with saline and patted dry with a paper towel, and all the blood vessels attached were also removed to minimize the potential contamination from blood and bile. Since the total volume of the biliary tree is quite small compared with the liver for both rat (0.5%) and human (0.3%) (Casali et al., 1994; Masyuk et al., 2001), the impact of bile contamination on liver concentration is likely to be small. Concentrations were determined using LC-MS/MS. Both pravastatin and its isomer (van Haandel et al., 2016), 3′α-hydroxy-pravastatin, were included in the calculation of K_{puu}. Free concentrations were calculated by multiplying the total plasma or total liver concentration by the f_u values of plasma or liver. The in vivo unbound liver-to-plasma ratio, K_{puu}, was obtained by dividing the steady-state unbound liver concentration by the unbound plasma concentration.

LC-MS/MS Quantification. A generic LC-MS/MS method is discussed here, and equivalent methods were also used based on compound properties. Two LC mobile phases were used: (A) 95% 2 mM ammonium acetate in water and 5% 50/50 methanol/acetonitrile and (B) 90% 50/50 methanol/acetonitrile and 10% 2 mM ammonium acetate in water, or (A) water with 0.1% formic acid and (B) acetonitrile with 0.1% formic acid. A flow rate of 0.5 ml/min was used with solvent gradient from 5% (B) to 95% (B) over 1.1 minutes to elute the compounds from the ultra-performance LC column (BEH C18, 1.7 μm, 50 × 2.1 mm; Waters, Milford, MA). The injection volume was 10 μl, and the cycle time was 2.5 minutes/injection. A CTC PAL autosampler (LEAP Technologies, Carrboro, NC), an model 1290 binary pump (Agilent, Santa Clara, CA) and an API 6500 triple quadrupole mass spectrometer with a TurboIonSpray source (AB Sciex, Foster City, CA) in MRM mode were used for sample analysis. Data collection processing and analysis were conducted with Analyst 1.6.1 software (Applied Biosystems, Foster City, CA).

Human in Vivo K_{puu} Estimation Based on PK/PD Modeling. The in vivo human K_{puu} values for rosuvastatin and pravastatin were calculated as the ratio between in vitro and in vivo IC_{50} values for 3-hydroxy-3-methylglutaryl-CoA reductase inhibition. The in vitro IC_{50} values were obtained from the literature (McTaggart et al., 2001; Holdgate et al., 2003; Gazzerro et al., 2012). The in vivo IC_{50} values were estimated using PK/PD modeling (Supplemental eq. 1). The rosuvastatin model published previously has adapted to estimate the in vivo IC_{50} in humans (Aoyama et al., 2010). This is a two compartment PK model developed with an indirect PD response incorporating circadian rhythm of mevalonic acid (MVA) production (Aoyama et al., 2010). Pravastatin plasma PK (Pan et al., 1990; van Luin et al., 2010) and plasma MVA concentrations in response to pravastatin (Nozaki et al., 1996) were used in the PK/PD modeling with the same

TABLE 1

Rat i.v. infusion experimental conditions

Compounds	Dose (mg/kg/h)	Dosing Vehicle
Cerivastatin	0.10	Saline
Fluvastatin	0.10	12% (w/v) SBECD in water
Rosuvastatin	0.10	12% (w/v) SBECD in water
Pravastatin	0.10	12% (w/v) SBECD in water
PF-04991532	0.12	PBS, pH 7.4
PF-05187965	1.2	12% (w/v) SBECD in water with 3 M equivalent 1N HCl

SBECD, sulfobutylether-β-cyclodextrin.

TABLE 2

In vivo rat i.v. infusion study for determination of liver-to-plasma K_{puu}

Compounds	Plasma Concentration at Terminal Time Point (ng/ml)	Liver Concentration at Terminal Time Point (ng/ml)	Total Liver-to-Plasma Ratio (K_p)	Rat Plasma $f_{u,p}$	Rat Liver $f_{u,liver}$	In Vivo Rat Liver-to-Plasma K_{puu}
Cerivastatin	261 ± 70	6717 ± 960	27 ± 8.0	0.016 ± 0.001	0.017 ± 0.001	29 ± 8.5
Fluvastatin	245 ± 34	8990 ± 1490	37 ± 7.4	0.011 ± 0.001	0.013 ± 0.001	44 ± 8.7
Rosuvastatin	14 ± 3.7	178 ± 50	13 ± 2.2	0.044 ± 0.009	0.19 ± 0.02	57 ± 9.5
Pravastatin	33 ± 19	171 ± 15	6.7 ± 4.5	0.54 ± 0.02	0.18 ± 0.02	2.2 ± 1.5
PF-04991532	172 ± 67	1170 ± 364	7.1 ± 2.0	0.12 ± 0.01	0.096 ± 0.02	5.7 ± 1.6
PF-05187965	76 ± 21	323 ± 13	4.4 ± 1.0	0.27 ± 0.01	0.15 ± 0.02	2.4 ± 0.57

method as rosuvastatin. All modeling was performed in NONMEM 7.2 (ICON Plc, Dublin, Ireland).

Calculation Methods. f_u was calculated with eq. 1 based on compound concentrations or area ratios between the test compound and the IS. For samples with diluted matrices, f_u was obtained with eqs. 2 and 3, where *D* is the dilution factor. The calculations of recovery and stability are shown in eqs. 4 and 5, respectively. In vitro K_{puu}, unbound cell concentration, and unbound medium concentration were obtained using eqs. 6–8.

$$f_u = \frac{\text{Receiver Concentration}}{\text{Donor Concentration}} \quad \text{Eq. (1)}$$

$$\text{Diluted } f_{u,d} = \frac{\text{Receiver Concentration}}{\text{Donor Concentration}} \quad \text{Eq. (2)}$$

$$\text{Undiluted } f_u = \frac{1/D}{\left(\left(1/f_{u,d}\right)-1\right)+1/D} \quad \text{Eq. (3)}$$

$$\%\ \text{Recovery} = \frac{\text{Donor Concentration} + \text{Receiver Concentration}}{\text{Donor Concentration at Time Zero}} \times 100\% \quad \text{Eq. (4)}$$

$$\text{Stability as } \%\ \text{Remaining} = \frac{\text{Concentration at Last Time Point}}{\text{Concentration at Zero Time Point}} \times 100\% \quad \text{Eq. (5)}$$

$$K_{puu} = \frac{C_{u,cell}}{C_{u,\ medium}} \quad \text{Eq. (6)}$$

$$C_{u,cell} = C_{total,cell} \times f_{u,cell} \quad \text{Eq. (7)}$$

$$C_{u,medium} = C_{total,medium} \times f_{u,medium} \quad \text{Eq. (8)}$$

Results

Development of IVIVE requires high-quality in vivo K_{puu} data to verify the in vitro results. As in vivo rat K_{puu} data can be obtained relatively easily by using i.v. infusion to ensure steady state has been achieved, K_{puu} IVIVE was first developed using the rat animal model. The method was then extended to humans, where quality in vivo K_{puu} data are quite limited. Four statins (cerivastatin, fluvastatin, rosuvastatin, and pravastatin) and two Pfizer internal liver-targeting compounds [PF-04991532 (Pfefferkorn et al., 2012) and PF-05187965 (Stevens et al., 2013)] were used for the study of rat IVIVE. All six compounds are OATP substrates consisting of a carboxylic acid functional group. Cerivastatin and pravastatin are OATP1B1 substrates; rosuvastatin and fluvastatin are substrates of OATP1B1, OATP1B3, and OATP2B1; and the two Pfizer compounds (PF-04991532 and PF-05187965) are substrates of OATP1B1 and OATP1B3 (University of Washington Drug-Drug Interaction Database, UCSF-FDA TransPortal) (Pfefferkorn et al., 2012; Stevens et al., 2013). The plasma and liver concentrations, measured at steady state, from in vivo rat i.v. infusion studies are shown in Table 2. K_{puu} was calculated based on in vivo liver-to-plasma K_p and in vitro $f_{u,p}$ and $f_{u,liver}$ from the equilibrium dialysis assay. The in vivo K_{puu} values of the compounds range from 2.2 to 57, covering a wide range of liver distribution properties. The in vitro K_{puu} data using cryopreserved suspension rat hepatocytes are summarized in Table 3. In vitro K_{puu} was calculated by multiplying in vitro K_p with $f_{u,cell}$ and dividing by $f_{u,media}$. Since $f_{u,cell}$ is similar to $f_{u,liver}$, as 80% of liver cells are hepatocytes (Bayliss and Skett, 1996), rat $f_{u,liver}$ data from Table 2 were used as $f_{u,cell}$ for the in vitro K_{puu} calculation. From this and previous studies (Riccardi et al., 2016), a 4-hour incubation time is a conservative time point to achieve a steady state in cells for most compounds. For example, the K_{puu} values for cerivastatin in rat hepatocytes were 39 ± 2.0, 34 ± 3.2, 24 ± 1.4, 31 ± 0.42, and 23 ± 2.3 at 1, 2, 3, 4 and 5 hours with 0.1 μM incubation, suggesting that a steady state has been achieved even after 1 hour of incubation. The comparison between in vitro K_{puu} from suspension rat hepatocytes and in vivo rat K_{puu} is shown in Table 4. A good correlation between in vitro and in vivo has been observed, and the K_{puu} values are mostly within 2-fold of each other. The lower K_{puu} value of pravastatin compared with the other three statins could potentially be due to higher biliary clearance, higher basolateral efflux, and lower active uptake. It appears that the drug-metabolizing enzymes and influx/efflux transporters are functioning at physiologic levels in the rat hepatocytes in suspension under the specific assay conditions. No scaling factors are necessary to predict in vivo K_{puu} data from in vitro data.

High-quality in vivo K_{puu} data from humans are very scarce. Liver biopsy is invasive and positron emission tomography (PET) imaging has a number of limitations (e.g., interference from metabolites, nonspecific binding to tissues at low doses). Nevertheless, a few in vivo human K_{puu} values are available to evaluate the in vitro K_{puu} method. Human liver PET data has been reported for [^{11}C]dehydropravastatin (DHP) (Shingaki et al., 2014). The K_{puu} was estimated to be 2.0 using terminal-phase (after 15 minutes) DHP data and in-house–measured pravastatin human $f_{u,p}$ (0.64) and $f_{u,liver}$ (0.17) values. It has been shown that the transporter and dispositional properties of DHP and pravastatin are very similar using an in vitro sandwich-cultured human hepatocyte assay and in vivo rat studies (Y. Sugiyama, personal communication).

TABLE 3

In vitro K_p and K_{puu} between cells and media in rat suspension hepatocytes

Compounds	$f_{u,media}$	$f_{u,cell}$[a]	K_p	K_{puu}
Cerivastatin	0.022 ± 0.003	0.017 ± 0.001	27 ± 2.6	21 ± 2.0
Fluvastatin	0.016 ± 0.001	0.013 ± 0.001	27 ± 1.8	22 ± 1.5
Rosuvastatin	0.19 ± 0.02	0.19 ± 0.02	35 ± 0.6	35 ± 0.6
Pravastatin	0.49 ± 0.06	0.18 ± 0.02	8.3 ± 0.8	3.0 ± 0.3
PF-04991532	0.12 ± 0.01	0.096 ± 0.02	8.9 ± 0.1	7.1 ± 0.1
PF-05187965	0.36 ± 0.01	0.15 ± 0.02	10 ± 0.4	4.2 ± 0.2

[a] $F_{u,cell}$ is assumed to be the same as $f_{u,liver}$ in Table 2, because 80% of the liver is made of hepatocytes by volume (Bayliss and Skett, 1996).

TABLE 4

Correlation between in vivo rat liver-to-plasma K_{puu} and in vitro suspension rat hepatocyte K_{puu}

Compounds	P_{app} MDCK-LE (10^{-6} cm/s)[a]	In Vivo Rat Liver-to-Plasma K_{puu}	In Vitro Suspension Rat Hepatocyte K_{puu}	Fold Difference in Vivo K_{puu}/In Vitro K_{puu}
Cerivastatin	10.3	29 ± 8.5	21 ± 2.0	1.4
Fluvastatin	7.8	44 ± 8.7	21 ± 1.5	2.1
Rosuvastatin	0.9	57 ± 9.5	35 ± 0.6	1.6
Pravastatin	0.4	2.2 ± 1.5	2.9 ± 0.3	0.8
PF-04991532	1.0	5.7 ± 1.6	7.1 ± 0.1	0.8
PF-05187965	0.5	2.4 ± 0.6	4.2 ± 0.2	0.6

MDCK-LE, Madin-Darby Canine Kidney-low efflux cell line; P_{app}, apparent permeability.
[a]P_{app} was measured using the MDCK-LE method (Di et al., 2011), and the values were obtained from the following references: Pfefferkorn et al. (2012), Stevens et al. (2013), and Varma et al. (2015).

Therefore, the K_{puu} value of DHP can be used as a surrogate for the K_{puu} value of pravastatin.

Because high-quality directly measured human in vivo K_{puu} data are fairly limited, human K_{puu} values of rosuvastatin and pravastatin were obtained indirectly using PK/PD modeling. Other statins were not included in the modeling due to the interference of active metabolites or insufficient literature data. The human in vivo liver-to-plasma K_{puu} of rosuvastatin was estimated to be 10. The average value reported in the literature for in vitro IC_{50} was 7 nM, ranging from 2 to 10 nM (McTaggart et al., 2001; Holdgate et al., 2003; Gazzerro et al., 2012). The in vivo IC_{50} of rosuvastatin was fitted to be 2.1 ng/ml with a 95 confidence interval (CI) of 1.87–2.32 ng/ml. The corresponding unbound IC_{50} was 0.7 nM (95% CI, 0.62–0.78 nM) using an in-house–measured $f_{u,p}$ of 0.16. The PK/PD model fits the data well (Supplemental Fig. 1), and the parameter estimates agree with those published previously (Supplemental Table 1) (Aoyama et al., 2010). The human in vivo liver-to-plasma K_{puu} of pravastatin was estimated to be 5.3. The average of the reported in vitro IC_{50} values was 48 nM ranging from 29 to 70 nM (Gazzerro et al., 2012). The in vivo IC_{50} of pravastatin was modeled to be 6.0 ng/ml with a 95% CI of 3.6–12.7 ng/ml, converting to an unbound in vivo IC_{50} of 9.0 nM (95% CI, 5.4–19.3 nM) based on an in-house–measured $f_{u,p}$ of 0.64. The modeling results are shown in Supplemental Table 2 and Supplemental Figure 2.

The comparison of human in vivo K_{puu} from PET or PK/PD modeling and in vitro K_{puu} from human hepatocytes in suspension is shown in Table 5. The in vitro assay predicted in vivo DHP K_{puu} values from PET data well (2.3 versus 2.0). The K_{puu} data from PK/PD modeling carry some uncertainties because it is an indirect in vivo measure of K_{puu} from many in vitro and in vivo parameters. Certain assumptions were made to obtain the K_{puu} values from PK/PD modeling. It is assumed that the in vitro assays fully capture the in vivo conditions and that the measured in vitro IC_{50} value can be directly used to quantitatively explain the PD (e.g., MVA) response to unbound liver drug concentrations. In addition, there are only eight and five time point measurements of plasma concentrations of MVA, respectively, in each group of the rosuvastatin and pravastatin studies, and only one PD study of each statin was available to be included in the analysis. Giving the uncertainty of the in vivo K_{puu} values from PK/PD modeling, it is reasonable that the in vitro K_{puu} data are within 2-fold and 4-fold of the in vivo K_{puu} estimates from PK/PD modeling. The human K_{puu} IVIVE is similar to that observed in the rat based on limited data, suggesting that the in vitro K_{puu} method with suspension hepatocytes is a suitable in vitro tool to predict in vivo K_{puu} under specific assay conditions. As more human in vivo K_{puu} data become available, the performance of the in vitro K_{puu} method will continue to be verified.

Discussion

Determination of the unbound liver concentration is critical to understand the pharmacology of disease targets in the liver, develop PK/PD relationships, predict DDI potentials, and anticipate liver toxicity. The ability to predict in vivo liver-to-plasma K_{puu} values from in vitro assays is highly desirable as there is no easy way to measure the human unbound liver concentration. With K_{puu} values, unbound liver concentrations can be estimated from unbound plasma concentrations, which can be readily measured. As reported in the literature, a direct translation of in vitro K_{puu} to in vivo K_{puu} can be challenging because transporter protein levels and functions in the in vitro systems are quite different than those in the in vivo systems (Roelofsen et al., 1995; Bow et al., 2008; Kimoto et al., 2012; Kunze et al., 2014; Morse et al., 2015; Vildhede et al., 2015). Typically, empirical scaling factors are needed to predict in vivo drug disposition from in vitro data (Jones et al., 2012; Li et al., 2014). The scaling factors are system dependent and can vary with assay conditions, such as cell culture time/media, plated versus suspension cells, BSA versus no proteins, cell types (transfected cells versus hepatocytes), and medium composition. However, under this specific assay condition with cryopreserved hepatocyte suspension in InVitroGRO HI media with 4% BSA, the transporters and enzymes appear to be functioning at the physiologic level. Good K_{puu} IVIVE has been observed in both rat and human without any scaling factors. Both the specific assay media and the physiologic amount of BSA (4%) in the assay are important to generate good K_{puu} IVIVE. This is the first time that an in vitro assay shows good prediction of in vivo K_{puu} for OATP substrates. Based on the extended clearance concept, K_{puu} is affected by intrinsic clearance of passive diffusion, active hepatic uptake, sinusoidal efflux, biliary excretion, as well as metabolism. Based on some literature data, cryopreserved suspended hepatocytes did not retain proper functional activity of efflux transporters. This was likely due to the internalization or downregulation of some transporters (Bow et al., 2008). However, the information is controversial in the literature, as efflux activity has been reported in suspension hepatocytes of multiple species including rat, human, dog, and monkey (Li et al., 2008). The mechanistic understanding of why this particular assay condition seems to perform better others requires further investigation.

The in vivo K_{puu} measures the unbound drug concentration between liver and arterial blood rather than liver blood. The liver blood has lower drug concentrations than arterial blood for high-extraction drugs. Theoretically, for compounds with high liver extraction, the in vivo

TABLE 5

Correlation between in vitro and in vivo K_{puu} for humans

Compounds	In Vivo Liver-to-Plasma K_{puu}	In Vitro Suspension Hepatocyte K_{puu}
Pravastatin[a]	2.0 (DHP, PET), 5.3 (PK/PD)	2.3 ± 0.2
Rosuvastatin[b]	10 (PK/PD)	39 ± 5.0

[a]Pravastatin human $f_{u,p}$ = 0.64 ± 0.16, $f_{u,liver}$ = 0.17 ± 0.02, $f_{u,media}$ = 0.49 ± 0.06.
[b]Rosuvastatin human $f_{u,p}$ = 0.16 ± 0.05, $f_{u,liver}$ = 0.31 ± 0.02, $f_{u,media}$ = 0.19 ± 0.02.

measured K_{puu} value will be lower than the in vitro experimental K_{puu} value. However, in practice, these differences have not been observed. The in vitro K_{puu} values are shown to be both higher and lower than the in vivo K_{puu} values. This could potentially be due to experimental variability from both in vitro and in vivo assays, making it difficult to detect the differences. This theoretical difference between in vivo and in vitro K_{puu} values appears to be inconsequential for K_{puu} IVIVE.

In this study, we observed good correlation between in vivo K_{puu} values from PK/PD modeling and in vitro K_{puu}. The in vivo K_{puu} was calculated as the IC_{50} ratio of 3-hydroxy-3-methylglutaryl-CoA inhibition between in vitro and in vivo values. The in vitro IC_{50} was measured using human liver microsomes. Assuming that the in vitro IC_{50} fully captures in vivo conditions (e.g., enzyme activity, substrate concentration, pH, and temperature), has no impact of transporters, and represents the intrinsic inhibitory activity, this measured in vitro IC_{50} should explain the in vivo effect directly if the intracellular unbound drug concentration in the liver is known. However, in the absence of liver drug concentration, the human in vivo IC_{50} was estimated using PK/PD modeling based on unbound plasma concentration. The unbound statin concentration in the liver can be higher than unbound plasma concentrations due to OATP active uptake. Therefore, the IC_{50} ratio between in vitro and in vivo values reflects the unbound drug concentration difference between liver and plasma and can be used as a surrogate for K_{puu}. This novel in vitro K_{puu} method provides a new tool to assess in vivo K_{puu} in drug discovery. The information is useful to estimate human unbound liver drug concentrations, predict efficacy, and model DDI risks for drugs that have active influx/efflux in the liver by transporters.

Acknowledgments

We thank Rui Li and Hugh Barton for useful discussion, and Larry Tremaine and Tess Wilson for their leadership and support.

Authorship Contributions

Participated in research design: Riccardi, Lin, Li, Niosi, Ryu, Hua, Atkinson, Kosa, Litchfield, Di.

Conducted experiments: Riccardi, Ryu, Hua.

Performed data analysis: Riccardi, Lin, Li, Niosi, Ryu, Hua, Atkinson, Kosa, Litchfield, Di.

Wrote or contributed to the writing of the manuscript: Li, Atkinson, Kosa, Di.

References

Aoyama T, Omori T, Watabe S, Shioya A, Ueno T, Fukuda N, and Matsumoto Y (2010) Pharmacokinetic/pharmacodynamic modeling and simulation of rosuvastatin using an extension of the indirect response model by incorporating a circadian rhythm. *Biol Pharm Bull* **33**: 1082–1087.

Badée J, Achour B, Rostami-Hodjegan A, and Galetin A (2015) Meta-analysis of expression of hepatic organic anion-transporting polypeptide (OATP) transporters in cellular systems relative to human liver tissue. *Drug Metab Dispos* **43**:424–432.

Bayliss MK and Skett P (1996) Isolation and culture of human hepatocytes, in *Human Cell Culture Protocols* (Jones GE ed) pp 369–389, Humana Press, Totowa, NJ.

Bow DAJ, Perry JL, Miller DS, Pritchard JB, and Brouwer KLR (2008) Localization of P-gp (Abcb1) and Mrp2 (Abcc2) in freshly isolated rat hepatocytes. *Drug Metab Dispos* **36**:198–202.

Casali AM, Siringo S, Sofia S, Bolondi L, Di Febo G, and Cavalli G (1994) Quantitative analysis of intrahepatic bile duct component in normal adult human liver and in primary biliary cirrhosis. *Pathol Res Pract* **190**:201–206.

Di L, Whitney-Pickett C, Umland JP, Zhang H, Zhang X, Gebhard DF, Lai Y, Federico, 3rdJJ, Davidson RE, Smith R, et al. (2011) Development of a new permeability assay using low-efflux MDCKII cells. *J Pharm Sci* **100**:4974–4985.

Gazzerro P, Proto MC, Gangemi G, Malfitano AM, Ciaglia E, Pisanti S, Santoro A, Laezza C, and Bifulco M (2012) Pharmacological actions of statins: a critical appraisal in the management of cancer. *Pharmacol Rev* **64**:102–146.

Hedaya MA (2012) *Basic Pharmacokinetics*, CRC Press, New York.

Holdgate GA, Ward WH, and McTaggart F (2003) Molecular mechanism for inhibition of 3-hydroxy-3-methylglutaryl CoA (HMG-CoA) reductase by rosuvastatin. *Biochem Soc Trans* **31**:528–531.

Ito S (2011) Pharmacokinetics 101. *Paediatr Child Health* **16**:535–536.

Jones HM, Barton HA, Lai Y, Bi YA, Kimoto E, Kempshall S, Tate SC, El-Kattan A, Houston JB, Galetin A, et al. (2012) Mechanistic pharmacokinetic modeling for the prediction of transporter-mediated disposition in humans from sandwich culture human hepatocyte data. *Drug Metab Dispos* **40**:1007–1017.

Kimoto E, Yoshida K, Balogh LM, Bi YA, Maeda K, El-Kattan A, Sugiyama Y, and Lai Y (2012) Characterization of organic anion transporting polypeptide (OATP) expression and its functional contribution to the uptake of substrates in human hepatocytes. *Mol Pharm* **9**:3535–3542.

Kunze A, Huwyler J, Camenisch G, and Poller B (2014) Prediction of organic anion-transporting polypeptide 1B1- and 1B3-mediated hepatic uptake of statins based on transporter protein expression and activity data. *Drug Metab Dispos* **42**:1514–1521.

Li M, Yuan H, Li N, Song G, Zheng Y, Baratta M, Hua F, Thurston A, Wang J, and Lai Y (2008) Identification of interspecies difference in efflux transporters of hepatocytes from dog, rat, monkey and human. *Eur J Pharm Sci* **35**:114–126.

Li R, Barton HA, Yates PD, Ghosh A, Wolford AC, Riccardi KA, and Maurer TS (2014) A "middle-out" approach to human pharmacokinetic predictions for OATP substrates using physiologically-based pharmacokinetic modeling. *J Pharmacokinet Pharmacodyn* **41**:197–209.

Masyuk TV, Ritman EL, and LaRusso NF (2001) Quantitative assessment of the rat intrahepatic biliary system by three-dimensional reconstruction. *Am J Pathol* **158**:2079–2088.

Mateus A, Matsson P, and Artursson P (2013) Rapid measurement of intracellular unbound drug concentrations. *Mol Pharm* **10**:2467–2478.

McTaggart F, Buckett L, Davidson R, Holdgate G, McCormick A, Schneck D, Smith G, and Warwick M (2001) Preclinical and clinical pharmacology of Rosuvastatin, a new 3-hydroxy-3-methylglutaryl coenzyme A reductase inhibitor. *Am J Cardiol* **87** (5A):28B–32B.

Morse BL, Cai H, MacGuire JG, Fox M, Zhang L, Zhang Y, Gu X, Shen H, Dierks EA, Su H, et al. (2015) Rosuvastatin liver partitioning in cynomolgus monkeys: measurement in vivo and prediction using in vitro monkey hepatocyte uptake. *Drug Metab Dispos* **43**:1788–1794.

Nozaki S, Nakagawa T, Nakata A, Yamashita S, Kameda-Takemura K, Nakamura T, Keno Y, Tokunaga K, and Matsuzawa Y (1996) Effects of pravastatin on plasma and urinary mevalonate concentrations in subjects with familial hypercholesterolaemia: a comparison of morning and evening administration. *Eur J Clin Pharmacol* **49**:361–364.

Pan HY, DeVault AR, Swites BJ, Whigan D, Ivashkiv E, Willard DA, and Brescia D (1990) Pharmacokinetics and pharmacodynamics of pravastatin alone and with cholestyramine in hypercholesterolemia. *Clin Pharmacol Ther* **48**:201–207.

Pfefferkorn JA, Guzman-Perez A, Litchfield J, Aiello R, Treadway JL, Pettersen J, Minich ML, Filipski KJ, Jones CS, Tu M, et al. (2012) Discovery of (S)-6-(3-cyclopentyl-2-(4-(trifluoromethyl)-1H-imidazol-1-yl)propanamido)nicotinic acid as a hepatoselective glucokinase activator clinical candidate for treating type 2 diabetes mellitus. *J Med Chem* **55**:1318–1333.

Prasad B, Evers R, Gupta A, Hop CECA, Salphati L, Shukla S, Ambudkar SV, and Unadkat JD (2014) Interindividual variability in hepatic organic anion-transporting polypeptides and P-glycoprotein (ABCB1) protein expression: quantification by liquid chromatography tandem mass spectroscopy and influence of genotype, age, and sex. *Drug Metab Dispos* **42**:78–88.

Riccardi K, Cawley S, Yates PD, Chang C, Funk C, Niosi M, Lin J, and Di L (2015) Plasma protein binding of challenging compounds. *J Pharm Sci* **104**:2627–2636.

Riccardi K, Li Z, Brown JA, Gorgoglione MF, Niosi M, Gosset J, Huard K, Erion DM, and Di L (2016) Determination of unbound partition coefficient and in vitro-in vivo extrapolation for SLC13A transporter-mediated uptake. *Drug Metab Dispos* **44**:1633–1642.

Roelofsen H, Bakker CTM, Schoemaker B, Heijn M, Jansen PLM, and Elferink RPJO (1995) Redistribution of canalicular organic anion transport activity in isolated and cultured rat hepatocytes. *Hepatology* **21**:1649–1657.

Rosenson RS (2003) Rosuvastatin: a new inhibitor of HMG-coA reductase for the treatment of dyslipidemia. *Expert Rev Cardiovasc Ther* **1**:495–505.

Scott DO, Ghosh A, Di L, and Maurer TS (2016) Passive drug permeation through membranes and cellular distribution. *Pharmacol Res* **117**:94–102.

Shingaki T, Tanaka M, Ishii A, Katayama Y, Tazawa S, Wada Y, Cui Y, Maeda K, Kusuhara H, Sugiyama Y, et al. (2014) Clinical evaluation of OATPs and MRP2 activity using positron emission tomography (PET) with [11C]dehydropravastatin, in *Proceedings of 19th North American ISSX Meeting/29th JSSX Meeting*; 2014 19–24 October, San Francisco, CA. Poster P430. International Society for the Study of Xenobiotics, Washington, DC.

Shitara Y, Horie T, and Sugiyama Y (2006) Transporters as a determinant of drug clearance and tissue distribution. *Eur J Pharm Sci* **27**:425–446.

Shitara Y, Maeda K, Ikejiri K, Yoshida K, Horie T, and Sugiyama Y (2013) Clinical significance of organic anion transporting polypeptides (OATPs) in drug disposition: their roles in hepatic clearance and intestinal absorption. *Biopharm Drug Dispos* **34**:45–78.

Smith DA, Di L, and Kerns EH (2010) The effect of plasma protein binding on in vivo efficacy: misconceptions in drug discovery. *Nat Rev Drug Discov* **9**:929–939.

Stevens BD, Litchfield J, Pfefferkorn JA, Atkinson K, Perreault C, Amor P, Bahnck K, Berliner MA, Calloway J, Carlo A, et al. (2013) Discovery of an intravenous hepatoselective glucokinase activator for the treatment of inpatient hyperglycemia. *Bioorg Med Chem Lett* **23**:6588–6592.

van Haandel L, Gibson KT, Leeder JS, and Wagner JB (2016) Quantification of pravastatin acid, lactone and isomers in human plasma by UHPLC-MS/MS and its application to a pediatric pharmacokinetic study. *J Chromatogr B Analyt Technol Biomed Life Sci* **1012-1013**:169–177.

van Luin M, Colbers A, van Ewijk-Beneken Kolmer EW, Verweij-van Wissen CP, Schouwenberg B, Hoitsma A, da Silva HG, and Burger DM (2010) Drug-drug interactions between raltegravir and pravastatin in healthy volunteers. *J Acquir Immune Defic Syndr* **55**:82–86.

Varma MV, Steyn SJ, Allerton C, and El-Kattan AF (2015) Predicting clearance mechanism in drug discovery: extended clearance classification system (ECCS). *Pharm Res* **32**:3785–3802.

Vildhede A, Wiśniewski JR, Norén A, Karlgren M, and Artursson P (2015) Comparative proteomic analysis of human liver tissue and isolated hepatocytes with a focus on proteins determining drug exposure. *J Proteome Res* **14**:3305–3314.

Watanabe T, Kusuhara H, and Sugiyama Y (2010) Application of physiologically based pharmacokinetic modeling and clearance concept to drugs showing transporter-mediated distribution and clearance in humans. *J Pharmacokinet Pharmacodyn* **37**:575–590.

Yabe Y, Galetin A, and Houston JB (2011) Kinetic characterization of rat hepatic uptake of 16 actively transported drugs. *Drug Metab Dispos* **39**:1808–1814.

Address correspondence to: Li Di, Pharmacokinetics, Dynamics and Metabolism, Pfizer Inc., Eastern Point Road, Groton, CT 06345. E-mail: li.di@pfizer.com

Supplementary Material

Novel Method to Predict *In Vivo* Liver-to-Plasma K_{puu} for OATP Substrates Using Suspension Hepatocytes

Keith Riccardi, Jian Lin, Zhenhong Li, Mark Niosi, Sangwoo Ryu, Wenyi Hua, Karen Atkinson, Rachel E. Kosa, John Litchfield, Li Di

Drug Metabolism and Disposition

Figure Legend

Figure S1. Plasma mevalonic acid (MVA) profiles in response to rosuvastatin. (A) plasma MVA profiles in healthy control subjects of morning dosing group ; (B) plasma MVA profiles in healthy control subjects of evening dosing group; (C) plasma MVA profiles in healthy subjects with rosuvastatin morning dose; (D) plasma MVA profiles in healthy subjects with rosuvastatin evening dose. LB: 95% lower prediction band; UB: 95% upper prediction band.

Figure S2. Plasma mevalonic acid (MVA) profiles in response to pravastatin. (A) plasma MVA profiles in healthy control subjects of morning dosing group ; (B) plasma MVA profiles in healthy control subjects of evening dosing group; (C) plasma MVA profiles in healthy subjects with pravastatin morning dose; (D) plasma MVA profiles in healthy subjects with pravastatin evening dose. LB: 95% lower prediction band; UB: 95% upper prediction band.

Table Legend

Table S1. Model Parameters of Rosuvastatin PK/PD modeling

Table S2. Model Parameters of Pravastatin PK/PD modeling

Table S1. Model Parameters of Rosuvastatin PK/PD modeling

Parameters	***Units***	***Estimates***	***SE%***	***Annotations***
CL	ml/min/kg	11.3	2.20	Plasma clearance
V1	L/kg	3.11	8.87	Volume of distribution in central compartment
Q12	ml/min/kg	6.81	26.0	Inter-compartment clearance
V2	L/kg	3.55	24	Volume of distribution in peripheral compartment
MAT	hour	2.48	9.19	Mean absorption time
Fa	-	0.2	-	Bioavailability, Fixed (Rosenson, 2003)
IC	ng/ml	4.75	2.01	Initial plasma concentration of MVA
Kamp	ng/ml/h	1.04	3.65	Amplitude of MVA production rate
tz	hour	16.4	0.787	Acrophase time of MVA synthesis rate
kout	1/hour	0.773	0.176	Elimination rate of MVA
IC50	ng/ml	2.09	3.57	IC50 of rosuvastatin based on its plasma concentration
γ	-	1.66	9.34	Hill coefficient

Rosenson RS (2003) Rosuvastatin: a new inhibitor of HMG-CoA reductase for the treatment of dyslipidemia. *Expert Review of Cardiovascular Therapy* **1:**495-505.

Table S2. Model Parameters of Pravastatin PK/PD modeling

Parameters	***Units***	***Estimates***	***SE%***	***Annotations***
CL	ml/min/kg	10.3	5.94	Plasma clearance
V1	L/kg	0.125	16.1	Volume of distribution in central compartment
Q12	ml/min/kg	6.63	15.5	Inter-compartment clearance
V2	L/kg	0.413	8.31	Volume of distribution in peripheral compartment
MAT	hour	1.79	2.21	Mean absorption time
Fa	-	0.18	-	Bioavailability, Fixed (Rosenson, 2003)
IC	pmol/mL	76.9	2.95	Initial plasma concentration of MVA
Kamp	pmol/ml/h	5.29	23.3	Amplitude of MVA production rate
tz	hour	14.1	2.05	Acrophase time of MVA synthesis rate
kout	1/hour	0.272	23.7	Elimination rate of MVA
IC_{50}	ng/mL	5.95	5.88	IC_{50} of rosuvastatin based on its plasma concentration
γ	-	1.35	34.2	Hill coefficient

Equation S1.

(Please refer to Tables S1 and S2 for symbol annotations)

PK equations:

$K_{10} = \frac{CL \times 60}{V_1 \times 1000}$ elimination rate constant from central compartment

$K_{12} = \frac{Q_{12} \times 60}{V_1 \times 1000}$ intercompartment clearance from central

$K_{21} = \frac{Q_{12} \times 60}{V_2 \times 1000}$ intercompartment clearance from peripheral

$K_a = \frac{1}{MAT}$ absorption rate constant

$\frac{d(Q_p)}{dt} = K_a \times Q_a - K_{10} \times Q_p - K_{12} \times Q_p + K_{21} \times Q_d$ derivative of plasma drug amount

$\frac{d(Q_d)}{dt} = K_{12} \times Q_p - K_{21} \times Q_d$ derivative of peripheral drug amount

$\frac{d(Q_a)}{dt} = -K_a \times Q_a$ derivative of drug amount for absorption

$C_p = \frac{Q_p}{V_1}$ plasma drug concentration

PD equations:

$K_m = K_{out} \times \mathrm{IC} - \frac{K_{amp} \times {K_{out}}^2 \times \left(\cos\left(\frac{2 \times \pi \times \mathrm{tz}}{24}\right) - \frac{2 \times \pi}{24 \times K_{out}} \times \sin\left(\frac{2 \times \pi \times \mathrm{tz}}{24}\right)\right)}{{K_{out}}^2 + \left(\frac{2 \times \pi}{24}\right)^2}$ mean MVA synthesis rate

$K_{in} = K_m + K_{amp} \times \cos\left(\frac{2 \times \pi \times (t - \mathrm{tz})}{24}\right)$ MVA synthesis rate

$\frac{d(MVA)}{dt} = K_{in} \times \left(1 - \frac{{C_p}^{\gamma}}{{IC_{50}}^{\gamma} + {C_p}^{\gamma}}\right) - K_{out} \times MVA$ derivative of plasma MVA

Figure S1. Plasma mevalonic acid (MVA) profiles in response to rosuvastatin. (A) plasma MVA profiles in healthy control subjects of morning dosing group ; (B) plasma MVA profiles in healthy control subjects of evening dosing group; (C) plasma MVA profiles in healthy subjects with rosuvastatin morning dose; (D) plasma MVA profiles in healthy subjects with rosuvastatin evening dose. LB: 95% lower prediction band; UB: 95% upper prediction band.

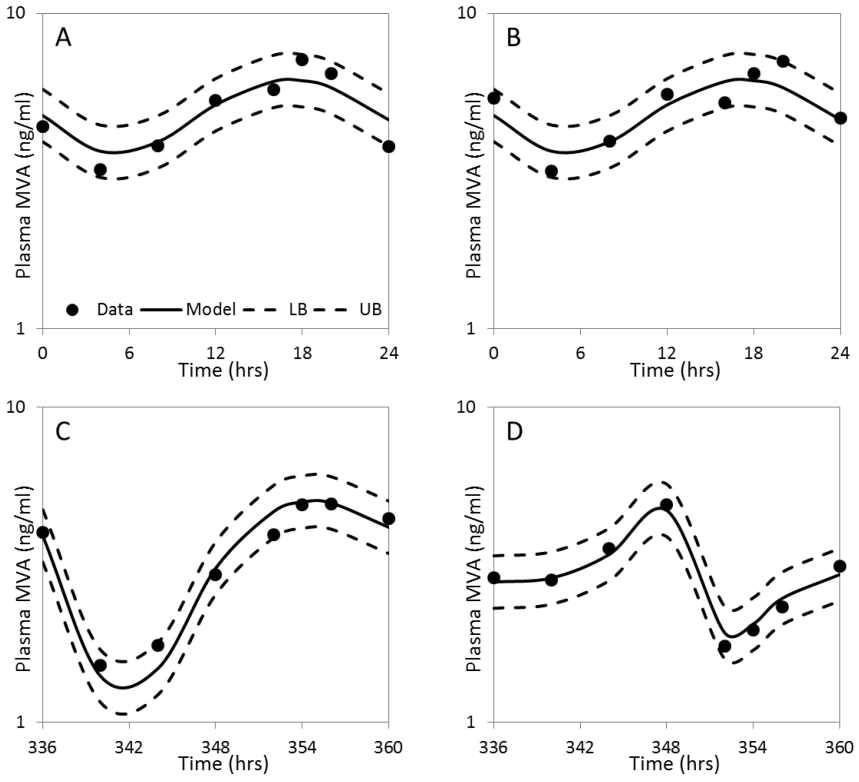

Figure S2. Plasma mevalonic acid (MVA) profiles in response to pravastatin. (A) plasma MVA profiles in healthy control subjects of morning dosing group ; (B) plasma MVA profiles in healthy control subjects of evening dosing group; (C) plasma MVA profiles in healthy subjects with pravastatin morning dose; (D) plasma MVA profiles in healthy subjects with pravastatin evening dose. LB: 95% lower prediction band; UB: 95% upper prediction band.